ROYAL SOCIETY OF CHEMISTRY

PAPER

CrossMark
← click for updates

Reversible CO exchange at platinum(0). An example of similar complex properties produced by ligands with very different stereoelectronic characteristics†

Sebastian J. K. Forrest, Paul G. Pringle,* Hazel A. Sparkes and Duncan F. Wass*

The ligands 1,2-C$_6$H$_4$(CH$_2$P^{t}Bu$_2$)$_2$ (**L$_a$**) and 1,2-C$_6$H$_4$(P^{t}Bu$_2$)(CH$_2$P^{t}Bu$_2$) (**L$_b$**) displace norbornene (nbe) from [Pt(η^2-nbe)$_3$] to give [PtL(η^2-nbe)] where L = **L$_a$** (**1a**) or **L$_b$** (**1b**); **1a** is fluxional on the NMR timescale. Reaction of **1a,b** with CO gives the corresponding monocarbonyls [PtL(CO)] where L = **L$_a$** (**2a**) or **L$_b$** (**2b**) which then react further, and reversibly, to give the dicarbonyls [PtL(CO)$_2$] where L = **L$_a$** (**3a**) or **L$_b$** (**3b**). The CO interchange between **2a,b** and **3a,b** is compared with the only other such system (**2f** and **3f**), which are complexes of (C$_2$F$_5$)$_2$PCH$_2$CH$_2$P(C$_2$F$_5$)$_2$ (**L$_f$**). Ethene reacts smoothly with **2a** to give (**4a**) and H$_2$ with **2a** generates some [PtH$_2$(**L$_a$**)]. Protonation of **2a** gives [Pt(**L$_a$**)(H)(CO)][B(C$_6$F$_5$)$_4$] (**5a**) whose crystal structure has been determined. Similarly protonation of **2b** gives [Pt(**L$_b$**)(H)(CO)][B(C$_6$F$_5$)$_4$] as a mixture of geometric isomers **5b−6b**.
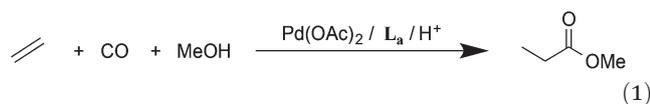
Introduction

The bulky *o*-xylenyl diphosphine **L$_a$** (Chart 1) was first prepared in 1976 by Shaw *et al.* who also reported *cis*-[PtH$_2$(**L$_a$**)], the first example of a *cis*-dihydridoplatinum(II) complex.[1] Spencer *et al.* later reported that treatment of complexes of the type [Pt(**L$_a$**)-(η^2-alkene)] with a Brønsted acid produced the first examples of β-agostic C–H–Pt complexes.[2,3] More recently, **L$_a$** has been used in the commercialised Pd-catalysed ethene hydromethoxy-carbonylation (Lucite Process) for the production of methyl methacrylate, shown in eqn (1).[4]

$$\diagup\diagup \quad + \quad CO \quad + \quad MeOH \quad \xrightarrow{\text{Pd(OAc)}_2 \text{/ } \mathbf{L_a} \text{/ H}^+} \quad \overset{O}{\diagup\diagdown}OMe$$

(1)

This application has galvanised academic interest in the Pd and Pt chemistry of **L$_a$** and related ligands (*e.g.* ligands **L$_b$**–**L$_e$** shown in Chart 1)[5–10] with the aim of understanding the special qualities of the **L$_a$** chelate. For example, using isotopically labelled MeOD and ^{13}CH$_2$=CH$_2$, Iggo *et al.*[6,7] identified by NMR the key intermediates in the carbonylation cycle with Pd–**L$_a$** and Pt–**L$_a$** catalysts; they determined that the Pt-catalysis

School of Chemistry, University of Bristol, Cantock's Close, Bristol BS8 1TS, UK.
E-mail: paul.pringle@bristol.ac.uk, duncan.wass@bristol.ac.uk
†CCDC 1015609. For crystallographic data in CIF or other electronic format see DOI: 10.1039/c4dt02303j
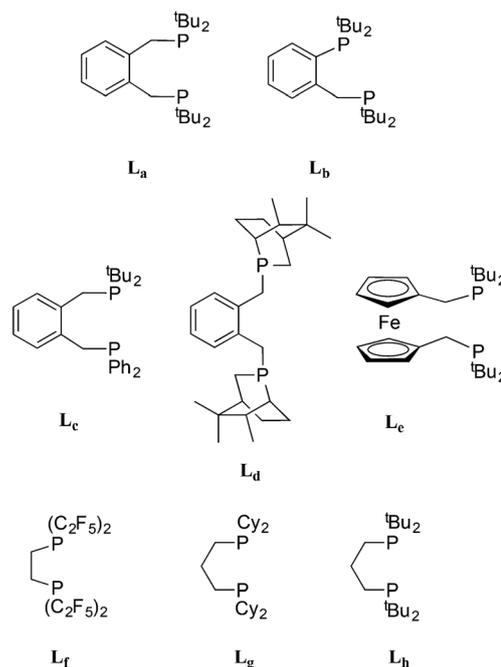
Chart 1 Structures of ligands discussed.

(Scheme 1) is inhibited by the reversible binding of CO to the Pt(II) intermediates while the corresponding Pd–**L$_a$** cycle is not similarly inhibited because of the lower affinity of Pd(II) for CO.
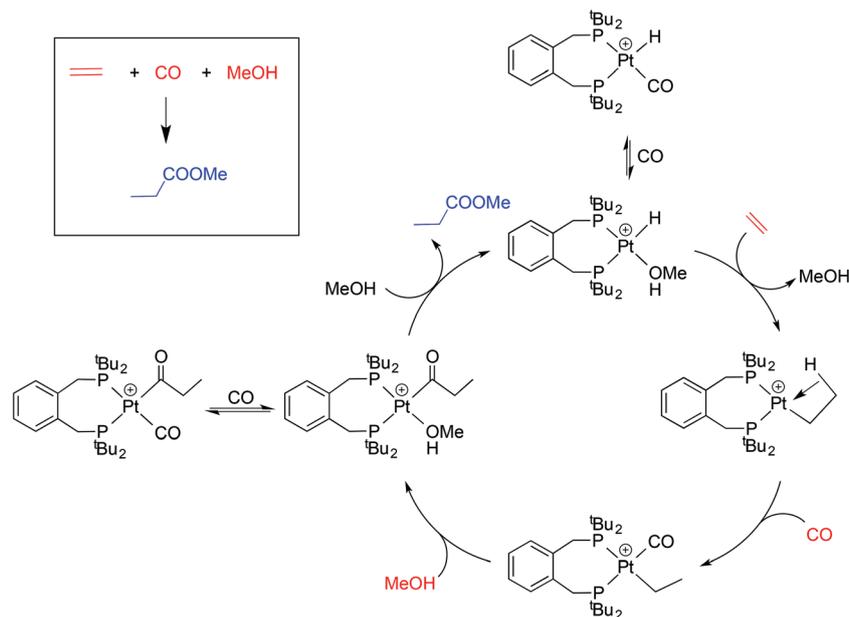
Scheme 1 Outline of the mechanism of Pt-catalysed hydromethoxycarbonylation of ethene[7] including two exocyclic equilibria.

It has been established that the activity and longevity of the Pd-catalyst for carbonylation can be improved by ligand modification.[6] For example, we have shown that changing the backbone from xylenediyl in L_a to toluenediyl in L_b led to a more active Pd-catalyst.[8] This has prompted us to investigate and compare the coordination chemistry of L_a and L_b, particularly that which may be relevant to the ethene hydromethoxycarbonylation catalysis (eqn (1)).[9]

The dichloroplatinum(II) complexes of L_a and L_b have been shown to be fluxional on the NMR timescale.[11] The conformations of the chelate rings in [PtCl$_2$(L)], as determined by X-ray crystallography, are depicted as **A** (L = L_a) and **B** (L = L_b) in Chart 2 and the observed fluxionality is associated with ring inversion.

Here we present the characterisation of Pt(0)–carbonyl complexes of the electron-rich, bulky ligands L_a and L_b, that have the property of reversible CO-interchange between three- and four-coordinate complexes, only previously observed with Pt(0)

complexes of the electron-poor L_f. The reactions of the carbonyl complexes of L_a and L_b with ethene, H_2 and H^+ are also described and the relevance of this chemistry to the carbonylation catalysis shown in Scheme 1 is discussed.

Results and discussion

The platinum(0) chemistry of L_a and L_b is summarised in Scheme 2. Addition of 1 equiv. of L_a or L_b to [Pt(η^2-nbe)$_3$] (nbe = norbornene) gave the corresponding [Pt(L)(η^2-nbe)] (**1a**, L = L_a; **1b**, L = L_b). The ^{31}P NMR spectrum of the previously reported[2] **1a** at −60 °C in toluene, showed 2 singlets in the ratio of *ca.* 7 : 3 (δ 49.2 ppm J_{PtP} = 3325 Hz and δ 47.3 ppm J_{PtP} = 3308 Hz) which coalesce at 0 °C, consistent with the interchange of the diastereoisomeric rotamers **1a** and **1a′** shown in eqn (2). The ^{1}H NMR spectrum of **1a** at −40 °C shows two multiplets for the diphos CH$_2$ which coalesce at −20 °C and appear as a broad singlet ($w_{1/2}$ = 23 Hz) at room temperature; only one A$_9$XX′ signal for the ^{t}Bu groups was discerned across the temperature range −40 to +20 °C indicating the insensitivity of this signal to the inequivalence of these groups. Two mechanisms can be postulated for the interchange shown in eqn (2): chelate ring inversion and Pt–nbe bond rotation. Both are plausible since there is precedent for Pt–L_a chelate ring inversion on the NMR timescale[8–11] and slow rotation about the Pt–nbe bonds in [Pt(L_d)(η^2-nbe)], a complex of the xylenediyl ligand L_d (Chart 1), has been observed.[12]
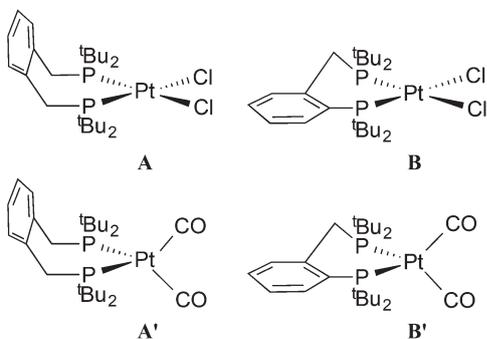
Chart 2 Conformations of the chelate rings in square planar (**A** and **B**) and tetrahedral (**A′** and **B′**) complexes.

$$(2)$$
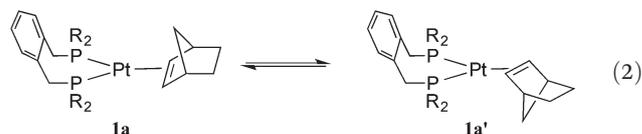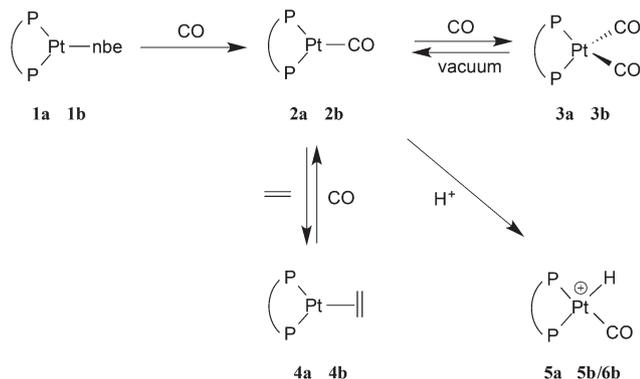
Scheme 2 When diphos = L_a, the complex is denoted *na*, and when diphos = L_b, the complex is denoted *nb*.

In the case of **1b**, its ^{31}P NMR spectrum shows sharp doublets over the whole temperature range of +23 to −90 °C which we interpret as due to there being a thermodynamic preference for one of the rotamers analogous to those shown in eqn (2). The ^1H NMR spectrum of **1b** showed 2 multiplets for the diphos CH_2 and 4 sharp A_9XX' multiplets for the ^tBu groups, consistent with the presence of a predominant isomer.

The displacement of the nbe from **1a** and **1b** to give the monocarbonyls **2a** and **2b** was achieved by bubbling CO through their toluene solutions and removing the solvent with the displaced nbe by evaporation to dryness. The colourlessness of **1a**/**1b** contrasts with the vivid orange-red of **2a**/**2b**.

Complexes **2a** and **2b** exhibit one $\nu(CO)$ band at 1907 and 1898 cm^{-1} respectively, (cf. for [Pt(PCy$_3$)$_2$(CO)], $\nu(CO)$ = 1916 cm^{-1}).[13] The ^{31}P NMR spectrum of **2a** shows the expected singlet at 70.0 ppm with a $^1J(PPt)$ of 3647 Hz and its ^1H NMR

spectrum shows one broad signal for the diphos CH_2 group and one A_9XX' multiplet for the ^tBu groups, as expected for a conformationally labile chelate.[8–10] Unexpectedly, the ^{31}P NMR spectrum of **2b** showed a single broad signal ($w_{1/2}$ = 40 Hz) at 78.5 ppm with $^1J(PPt)$ of 3450 Hz which below −20 °C is resolved into an AB pattern with δ 77.9 and 76.4, $^2J(PP)$ = 93 Hz and $^1J(PPt)$ = 3556 and 3250 Hz respectively (see Fig. 1).

The labelled compounds [Pt(L)(^{13}CO)] (**2a***, L = L_a; **2b***, L = L_b) were prepared in order to confirm their structures and to probe further the apparent fluxionality of **2b**. Treatment of **2a** and **2b** with ^{13}CO gave the labelled complexes **2a*** and **2b***. The ^{31}P NMR spectrum of **2a*** at ambient temperature is a doublet with $^2J(PC)$ = 45 Hz and its ^{13}C NMR spectrum shows a triplet at 229 ppm with $^1J(PtC)$ = 2096 Hz and the same $^2J(PC)$ of 45 Hz; these spectra support the monocarbonyl structure assigned to **2a**. The ^{31}P NMR spectrum of **2b*** at −90 °C showed an ABX pattern with ^{195}Pt satellites (see Fig. 1) and its ^{13}C NMR spectrum showed a doublet of doublets at 235 ppm with $^2J(PC)$ = 52 and 41 Hz and $^1J(PtC)$ = 2136 Hz; again, these spectra are consistent with the monocarbonyl structure assigned to **2b**. The ambient temperature ^{31}P and ^{13}C NMR spectra of **2b*** resembled the spectra for the unlabelled **2b**, being broad and unresolved. Above room temperature, the ^{31}P NMR spectrum of **2b*** broadens progressively until at +100 °C, $w_{1/2} \sim$ 400 Hz. In the ^{13}C NMR spectra of **2b*** measured between +40 and +100 °C, no CO signal was observed at all presumably because of its broadness. When the high temperature NMR samples were cooled to ambient temperature, the ^{31}P and ^{13}C NMR spectra reassumed their original forms.

It is not obvious what the source of the line-broadening is in the ^{31}P and ^{13}C NMR spectra of **2b** at ambient temperature and above. If the conformation of the 6-membered chelate in **2b** is **B/B′**-like (see Chart 2), then **2b** would exist as a pair of
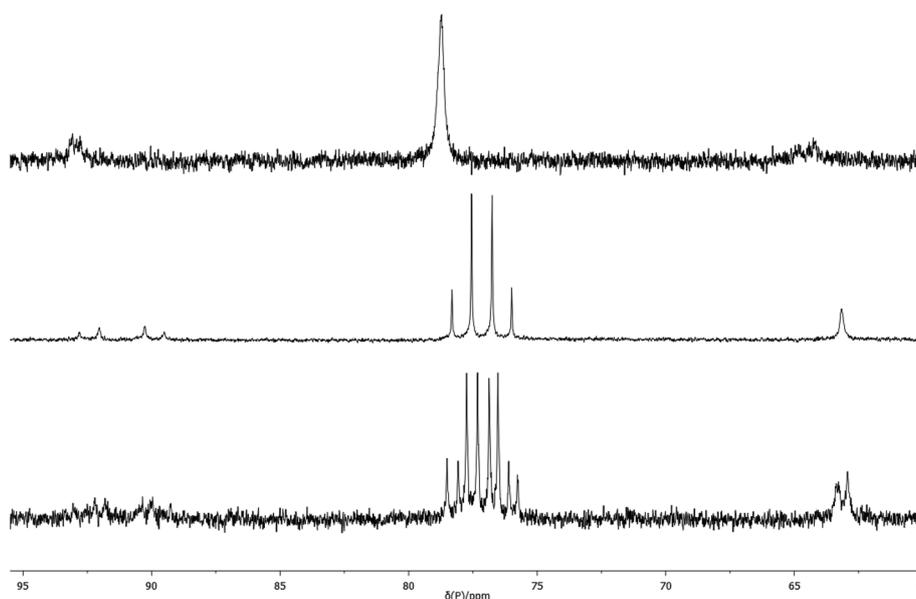
Fig. 1 Variable temperature ^{31}P NMR spectra: top, **2b**, room temperature; middle, **2b**, −90 °C; bottom, **2b***, −90 °C.

enantiomers (with identical ^{31}P shifts) and therefore interchange between such conformers would not contribute to the line broadening. If intermolecular CO exchange were taking place, P–C coupling would be lost in the labelled **2b*** which apparently it is, but this observation is inconclusive because the large observed NMR line-width would swamp the ^2J(PC) of 52 and 41 Hz (measured at −90 °C). Nevertheless, one explanation for the NMR behaviour is that at elevated temperatures, CO exchange is taking place perhaps *via* an analogue of $[Pt_2(CO)(\mu\text{-}CO)(L_g)_2]$ (see Chart 1 for structure of L_g) reported by Mezailles *et al.*[14] which is in equilibrium with **2b**.

The dicarbonyl complexes, $[PtL(CO)_2]$ (**3a**, L = L_a; **3b**, L = L_b) were generated when solutions of **2a** and **2b** were pressurised with 2 atm of CO. The solid state IR spectrum of **3a** showed ν(CO) bands at higher frequencies (1971 and 1931 cm^{-1}) than the 1907 cm^{-1} for **2a**, consistent with the two CO ligands in **3a** sharing the electron density from the platinum(0). The ^{31}P NMR spectrum of **3a** at room temperature showed no discernable resonances but at −90 °C, a singlet at 35.3 ppm with ^1J(PPt) of 3107 Hz was observed. At +40 °C, the only ^{31}P NMR signal observed was for **2a**, showing that CO dissociation from **3a** occurs readily and this explains the great broadness of the signal at ambient temperatures. The labelled complex $[Pt(L_a)(^{13}CO)_2]$ (**3a***) was prepared from **3a** and ^{13}CO and its ^{13}C NMR spectrum at −90 °C had multiplets at 187.1 and 186.6 ppm with ^1J(CPt) of 1832 and 1900 Hz respectively which were assigned to inequivalent Pt–CO ligands. The ^2J(CP) coupling was approximately 4 Hz, leading to multiplets in the ^{31}P and ^{13}C NMR spectra. The inequivalence of the CO ligands detected in the low temperature ^{13}C NMR spectrum of **3a*** is consistent with an **A′**-type conformation of the 7-membered chelate (see Chart 2) giving rise to CO ligands being *syn* and *anti* to the phenylene of the chelate.

The solid state IR spectrum of **3b** showed ν(CO) bands at higher frequencies (1961 and 1915 cm^{-1}) than the 1898 cm^{-1} in **2b**. The ^{31}P NMR spectrum of **3b** at ambient temperatures showed 2 sets of broad singlets at 44.4 and 42.7 ppm with ^1J(PPt) = 3106 and 3818 Hz respectively. The ^{13}C NMR spectrum of the labelled complex $[Pt(L_b)(^{13}CO)_2]$ (**3b***) had two signals at 187.1 and 186.0 ppm with ^1J(CPt) of 1930 and 1850 Hz respectively; the C–P coupling was not resolved in the ^{31}P or ^{13}C NMR spectra of **3b***. According to solid-state IR spectroscopy (see Fig. 2), when red solid monocarbonyl **2b** was subjected to a CO atmosphere, it was converted to yellow **3b** and this was reversed upon application of a vacuum to powdered **3b**.

Dissociation of CO from the dicarbonyls **3a/3b** to give **2a/2b** occurred slowly when their solutions were stirred under a N$_2$ atmosphere and rapidly when solutions were put under vacuum, presumably due to the dissolved CO being removed under the reduced pressure. The uptake of CO by **2a/2b** (eqn (3)) is notable because of its rarity[13] and reversibility.[14] There are several examples of 18-electron complexes of the type $[Pt(CO)_2(PR_3)_2]$[13,15] and $[Pt(CO)_2(diphos)]$[14,16] including the complex where diphos = L_h[17] (see Chart 1) which has ν_{CO} values (1912, 1960 cm^{-1}) closely similar to those for **3b**
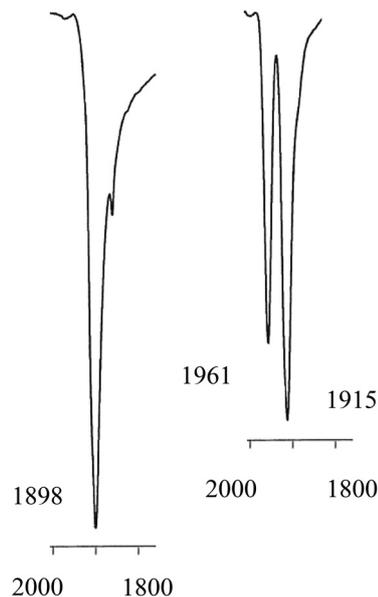
Fig. 2 Solid state IR spectra in the ν(CO) region for monocarbonyl **2b** (left) and dicarbonyl **3b** (right).

(see eqn (3)); the bulk and bite angles of L_h and L_b should be similar. However there is only one previously reported example of a 16-electron $[Pt(CO)(diphos)]$ complex, **2f**, which Roddick *et al.*[18] reported undergoes a similar CO interchange between **2f** and **3f** (eqn (3)). The explanation that was given for the stability of **2f** relative to **3f** was that the high π-acceptor capacity of the fluorophos ligand L_f efficiently delocalises the electron-density on the Pt(0); this is supported by the high ν_{CO} values for **2f** and **3f** (see eqn (3)). A similar argument is not tenable for **2a/2b** since L_a/L_b are strong σ-donors, as reflected in the low ν_{CO} values for their carbonyl complexes (see eqn (3)). The stability of the coordinatively unsaturated **2a/2b** is therefore associated with the large bulk of L_a/L_b. This steric argument can be extended to explain why CO dissociation from **3a** appears to be more facile than from **3b**, since L_a is more sterically demanding than L_b.[11] The complementary explanations for the equilibria shown in eqn (3) for $L_{a,b}$ *vs.* L_f exemplify how ligands with very different stereoelectronic properties can produce complexes with similar properties.

	ν_{CO} /cm^{-1}			ν_{CO} /cm^{-1}	
2a	1907	L_a	**3a**	1971	1931
2b	1898	L_b	**3b**	1961	1915
2f	2044	L_f	**3f**	2073	2038

(3)
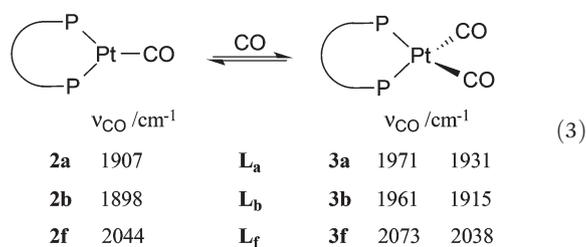
When a toluene solution of **2a** was stirred under an atmosphere of H$_2$ for 5 days, the *cis*-$[PtH_2(L_a)]$ was formed in approximately 50% NMR yield (along with other uncharacterised products), as shown by the close matching of the NMR data

(^{1}H: δ −3.8 ppm, J_{PtH} = 1004 Hz; ^{31}P: δ 45.7 ppm, J_{PtP} = 2109 Hz) with the literature values for this compound.[1]

The CO ligands in **2a** were displaced by ethene to give **4a** by repeated vacuum/ethene-addition cycles (see Experimental) and this transformation was readily reversed by the application of a CO atmosphere to **4a** (Scheme 2). Complex **4a** was characterised by matching of the NMR data with those previously reported for this complex.[19] Under similar conditions to those used to generate **4a**, **2b** reacted with ethene but the product, according to the ^{31}P NMR spectrum at −90 °C, was a mixture containing **2b** (50%), **3b** (30%) and a third species (20%) whose ^{31}P NMR parameters (60.9 with ^1J(PPt) = 3288 Hz, ^2J(PP) = 45 Hz; 57.9 ^1J(PPt) = 3288 Hz) led us to tentatively assign this minor product to **4b**, although we have not isolated it.

In the carbonylation catalytic cycle shown in Scheme 1, neutral species are not involved in the core cycle because the reaction is carried out in an acidic medium. For this reason, we investigated the protonation of the monocarbonyl complex **2a**. Treatment of the monocarbonyl complex **2a** with 1 equivalent of [[(Et$_2$O)$_2$H][B(C$_6$F$_5$)$_4$][20] in chlorobenzene gave a product assigned structure **5a** (Scheme 2) on the basis of its ^{1}H NMR spectrum which showed a signal at −4.7 ppm with J(PtH) = 736 Hz characteristic of a hydride. A band at 2092 cm^{-1} in its IR spectrum is typical of a cationic Pt(II)–CO.[21] The NMR spectroscopic data for **5a** match well those reported by Iggo et al.[7] for the triflate salt of **5a** which they characterized in solution only.

Crystals of **5a** suitable for X-ray crystallography grew from its CH$_2$Cl$_2$ solution, crystallising in the triclinic space group $P\bar{1}$ with two [Pt(L$_a$)(H)(CO)][B(C$_6$F$_5$)$_4$] moieties in the asymmetric unit, i.e. Z' = 2. Both of these moieties have essentially the same geometrical conformation and selected bond lengths and angles are listed below Fig. 3. The location of the hydride was not determined directly from the data, but its position was inferred from the metal geometry and located accordingly. The P1–Pt1–P2 bite angle is 104.00(12)° and the P3–Pt2–P4 bite angle is 104.74(12)° and all four of the half cone angles are ∼117°.

The chelate conformations for xylenediyl diphos chelates can be described in terms of the two M–P–C–C(Ph) torsion angles. There are currently 12 Pt and 26 Pd xylenediyl diphos chelates in the Cambridge Crystallographic Database (CSD)[22], 35 of which have structures where the two M–P–C–C(Ph) torsion angles have similar absolute values and the ring conformation is half-chair-like with an essentially coplanar MP$_2$C$_2$ component as depicted as **A** in Chart 2. In the remaining 3 structures (HUXCIN,[23] HUXCEJ[23] and IHETOF[24]) the chelate rings adopt a twist-boat-like conformation, with two different Pt–P–C–C(Ph) torsion angles of approximately ±50° and ±14°. The conformation of the Pt–L$_a$ ring in **5a** (see Fig. 3) matches the majority of those in the CSD, with Pt–P–C–C(Ph) torsion angles for Pt1 of −54.5(12)° and 65.0(11)° and for Pt2 of 57.9 (11)° and −57.7(11)°.

Protonation of **2b** gave a mixture of geometric isomers of hydridocarbonyl complexes where the position of the H ligand relative to the P-aryl is cis (**5b**) or trans (**6b**). Evidence for the two isomers in solution comes from the ^{1}H NMR spectrum which showed 2 hydride signals at −2.3 and −4.3 ppm in a 1 : 4 ratio and the ^{31}P NMR spectrum showed two sets of signals; the NMR data for the two species are similar and therefore it was not possible to assign the major isomer (see Experimental for the data). The solid state IR spectrum of the **5b**–**6b** mixture shows 2 ν(CO) bands at 2102 and 2094 cm^{-1}.

5b **6b**
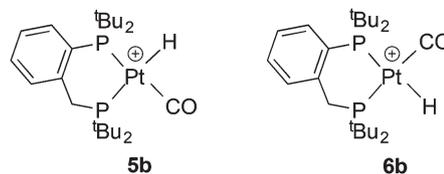
Conclusion

We have shown here that the mono- and dicarbonylplatinum(0) complexes **2a**/**2b** and **3a**/**3b** are readily formed and interconvert.
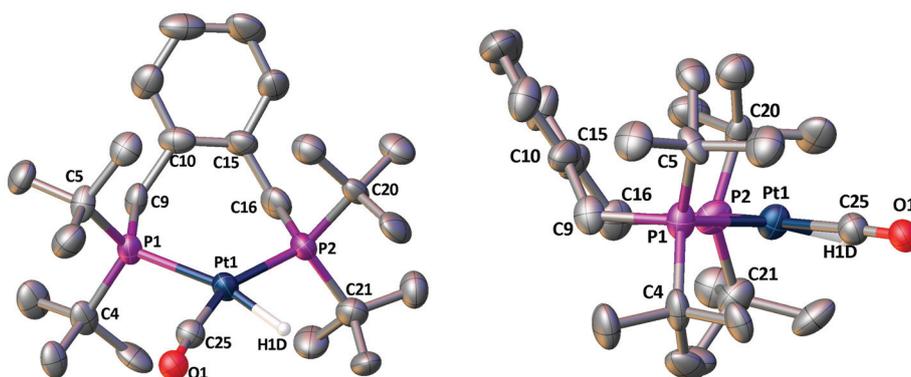
Fig. 3 Crystal structure of [Pt(L$_a$)(H)(CO)][B(C$_6$F$_5$)$_4$] (**5a**). The view on the right shows the chelate ring conformation. Only one of the two Pt-containing moieties in the asymmetric unit is shown and only one position of the disordered CO/H combination. For clarity all of the hydrogen atoms (apart from the hydride H1D) are omitted along with the [B(C$_6$F$_5$)$_4$] counterions. Selected bond lengths (Å) and angles (°): Pt1–P1 2.366(3); Pt1–P2 2.328(3); Pt1–C25 1.900(14); Pt1–H1D 1.660(3); P1–C4 1.886(13); P1–C5 1.869(12); P1–C9 1.818(11); P2–C16 1.835(13); P2–C20 1.888(12); P2–C21 1.886(14); P1–Pt1–P2 104.00(12); C25–Pt1–P1 98.4(5); C25–Pt1–P2 157.5(5).

Scheme 3 Potential role for complexes **2–5** in the Pt-catalysed methoxycarbonylation mechanism.

The stability of the coordinatively unsaturated [Pt(CO)(diphos)] species **2a/2b** relative to **3a/3b** is associated with the steric congestion provided by the bulky diphos ligands **L$_a$** and **L$_b$**. The only related [Pt(CO)$_n$(diphos)] species reported (**2f/3f**) feature the electron-poor fluorinated diphos ligand **L$_f$** (which has modest steric bulk)[25] where the explanation given for the stability of the monocarbonyl is electronic – the π-acceptor properties of the diphos ligand destabilises the corresponding [Pt(CO)$_2$(diphos)]. This is a textbook example of ligands with very different stereoelectronic properties producing similar outcomes in terms of the properties of their complexes.

The hydromethoxycarbonylation of ethene is efficiently catalysed by Pd-complexes of **L$_a$** and **L$_b$** and Iggo *et al.*[7] have shown that the analogous organoplatinum chemistry is relevant in the study of the mechanism of the catalysis. Ethene reacts with the coordinatively unsaturated **2a** to give **4a** presumably *via* the 18-electron tetrahedral intermediate **X** (Scheme 3). The protonation of the **2a/2b** to give the cationic hydridocomplexes **5a/5b** (and the geometric isomer **6b**) is pertinent because the catalysis is carried out at low pH. It is possible that complexes of the type **2–5** described above are present in non-productive equilibria during the Pt-catalysed carbonylation shown in Scheme 1; their place is shown in Scheme 3.

Experimental

Unless otherwise stated, all reactions were carried out using standard Schlenk line and dry box techniques. Dry N$_2$-saturated solvents were collected from a Grubbs system in flame and vacuum-dried glassware. Deuterated solvents were dried and distilled from CaH$_2$. Pentane was dried over 4 Å molecular sieves and N$_2$-saturated by repeated freeze, vacuum and thawing cycles. The complex [Pt(η^2-nbe)$_3$][26] was prepared by literature methods. Ligand **L$_a$** was obtained from Lucite International. Ligand **L$_b$** was prepared as previously described.[11] CO, C$_2$H$_4$ and H$_2$, were used as obtained from BOC and ^{13}CO was used as obtained from Aldrich. NMR spectra were recorded on a Jeol ECP (Eclipse) 300 or a Varian VNMR S500 spectrometer. Chemical shifts are referenced relative to high frequency of Si(CH$_3$)$_4$ (^{1}H or ^{13}C), 85% H$_3$PO$_4$ (^{31}P), and CF$_3$Cl (^{19}F). Infrared spectra were obtained using a Perkin Elmer 1600 series FTIR. Mass spectrometry was carried out by the Mass Spectrometry Service at the University of Bristol. Elemental analyses were carried out by the Microanalytical Laboratory at the University of Bristol.

Preparation of [Pt(L$_a$)(η^2-nbe)] (1a)

This was made according to the method of Spencer *et al.* and characterised by comparison of the NMR spectra with the reported data.[2] The spectra at low temperature have not been previously reported. ^{31}P{H} NMR (202 MHz, C$_6$D$_5$CH$_3$, −60 °C): δ 49.2 (s, ^{1}J(PtP) = 3251 Hz), δ 47.3 (s, ^{1}J(PtP) = 3308 Hz).

Preparation of [Pt(L$_b$)(η^2-nbe)] (1b)

A solution of **L$_b$** (0.089 g, 0.26 mmol) in toluene (5 mL) was added in one portion to a solution of [Pt(η^2-nbe)$_3$] (0.125 g, 0.262 mmol) in toluene (5 mL) at −78 °C and the resulting mixture was stirred for 2 h, allowed to warm to room temperature and then stirred for a further 16 h. The volatiles were then removed under reduced pressure to yield an off-white solid that was dissolved in pentane (1 mL) and the product crystallized at −78 °C. The supernatant was removed by cannula and the white solid dried under vacuum (0.149 g, 0.222 mmol,

86%). Elemental analysis (calcd for $C_{30}H_{52}P_2Pt$): C: 54.17 (53.80) H: 7.83 (7.39). ESI accurate mass spectrum: (calcd for $C_{30}CH_{52}P_2Pt$ 669.3190) M_r − 669.3184. $^{31}P\{H\}$ NMR (202 MHz, C_6D_6): δ 63.9 (d, $^1J(PPt)$ = 3157 Hz, $^2J(PP)$ = 45 Hz), 57.6 (d, $^1J(PPt)$ = 3192 Hz, $^2J(PP)$ = 45 Hz). ^1H NMR (500 MHz, CD_2Cl_2): δ 7.1–6.9 (m, 4H), 3.3 (m, 2H, PCH_2), 3.1 (m, 2H, CCH), 2.5–2.2 (m, 2H, $PtCH$), 2.0 (m, 2H, $CCHH$), 1.7 (m, 2H, $CCHH$), 1.4 (d, $^3J(PH)$ = 13 Hz, 9H, CCH_3), 1.3 (d, $^3J(PH)$ = 13 Hz, 9H, CCH_3), 1.2 (d, $^3J(PH)$ = 12 Hz, 9H, CCH_3), 1.1 (d, $^3J(PH)$ = 12 Hz, 9H, CCH_3), 0.8 (m, 1H, CHH bridge), 0.7 (m, 1H, CHH bridge).

Preparation of [Pt(L$_a$)(CO)] (2a)

A solution of **L$_a$** (0.158 g, 0.415 mmol) in toluene (5 mL) was added in one portion to a solution of $[Pt(\eta^2\text{-nbe})_3]$ (0.198 g, 0.415 mmol) in toluene (5 mL) at −78 °C, the resulting mixture was stirred for 2 h, allowed to warm to room temperature and then stirred overnight. CO was then bubbled through the solution for 30 min to give an orange solution which was filtered and then the volatiles removed under reduced pressure. The residue was redissolved in toluene (5 mL) and CO was bubbled through solution again. The vacuum/CO cycle was repeated twice more to ensure that all norbornene had been displaced. The solvent was then removed under reduced pressure and the solid extracted with pentane (3 × 5 mL). The volume of the solution was reduced to 3 mL and the product crystallised at −78 °C. The supernatant was removed by cannula and the orange solid dried under vacuum (0.146 g, 0.238 mmol, 58%). Elemental analysis (calcd for $C_{25}H_{44}OP_2Pt$, $0.5C_5H_{12}$): C: 50.46 (50.53) H: 7.41 (7.71). ESI accurate mass spectrum: (calcd for $C_{25}H_{44}OP_2Pt$ 617.2513) M_r − 617.617.2532. IR: ν_{CO} 1907 cm^{-1}. $^{31}P\{H\}$ NMR (162 MHz, C_6D_6): δ 70.2 (s, $^1J(PPt)$ = 3647 Hz). ^1H NMR (500 MHz, C_6D_6): δ. 7.1 (m, 2H,), 6.9 (m, 2H), 3.5 (br, 4H, CH_2), 1.2 (m, 36H. CH_3). $^{13}C\{H\}$ NMR (101 MHz, C_6D_6): δ 137.9 (s), 133.7 (s), 125.6 (s), 36.8 (br, CH_2), 32.3 (m, CCH_3,), 29.9 (m, CCH_3).

Preparation of [Pt(L$_a$)(^{13}CO)] (2a*)

A solution of **2a** (9.4 mg, 0.015 mmol) in d_6-benzene (1.2 mL) was placed in a valved NMR tube. The solution was frozen with liquid N_2 and then the NMR tube was evacuated and sealed. The solution was then thawed and the NMR tube backfilled with ^{13}CO (2 bar) and the resulting mixture allowed to react for 30 min. The vacuum/CO cycle was repeated twice more to ensure that most of the ^{12}CO had been displaced. The solution was then saturated with N_2 and the product was identified in solution by NMR only. The ^1H NMR spectrum of **2a*** was essentially the same as for **2a**. $^{31}P\{H\}$ NMR (121 MHz, C_6D_6): δ 70.2 (d, $^1J(PPt)$ = 3647 Hz, $^2J(PC)$ = 45 Hz). $^{13}C\{H\}$ NMR (101 MHz, C_6D_6): δ 228.9 (t, $^2J(CP)$ = 45 Hz, CO), $^1J(CPt)$ = 2100 Hz).

Preparation of [Pt(L$_b$)(CO)] (2b)

CO was bubbled through solution a solution of **1b** (0.135 g, 0.202 mmol) in toluene (10 mL) for 30 min to give a yellow solution which was filtered and then the volatiles removed under reduced pressure. The residue was redissolved in

toluene (5 mL) and CO was bubbled through the solution again. The vacuum/CO cycle was repeated twice more to ensure that all of the norbornene had been displaced. The solvent was removed under reduced pressure to give a yellow solid which turned red under prolonged exposure to vacuum. The solid was extracted with pentane (3 mL) and the product crystallized at −78 °C. The supernatant was removed via cannula and the red solid dried under vacuum (0.108 g, 0.179 mmol, 88%). Elemental analysis (calcd for $C_{24}H_{42}OP_2Pt$, $0.5C_5H_{12}$): C: 50.19 (49.76) H: 7.75 (7.56). ESI accurate mass spectrum: (calcd for $C_{24}H_{43}OP_2Pt$ 604.2434) M_r +1−604.2431. IR: ν_{CO} 1898 cm^{-1}. $^{31}P\{H\}$ NMR (202 MHz, C_6D_6): δ 78.5 (br, $^1J(PPt)$ = 3450 Hz). δ 77.9 (d, $^1J(PPt)$ = 3556 Hz, $^2J(PP)$ = 93 Hz), 76.4 (d, $^1J(PPt)$ = 3250 Hz, $^2J(PP)$ = 93 Hz). $^{31}P\{H\}$ NMR (121 MHz, $C_6D_5CD_3$, −90 °C): δ 77.9 (dd, $^1J(PPt)$ = 3556 Hz, $^2J(PP)$ = 93 Hz), 76.4 (dd, $^1J(PPt)$ = 3250 Hz, $^2J(PP)$ = 93 Hz). ^1H NMR (400 MHz, C_6D_6): δ 7.8 (m, 1H), 7.1–6.9 (m, 3H), 3.2 (m, 2H, CH_2), 1.3–1.1 (m, 36H, CCH_3). $^{13}C\{H\}$ NMR (101 MHz, C_6D_6): δ 134.6 (m), 129.0 (m), 128.9 (s), 128.8 (s), 125.6 (s), 125.0 (m), 35.7 (br, CH_2), 30.9 (br, CCH_3), 29.3 (br, CCH_3).

Preparation of [Pt(L$_b$)(^{13}CO)] (2b*)

A solution of **2b** (11.2 mg, 0.0185 mmol) in benzene (1.2 mL) was placed in a valved NMR tube. The solution was frozen with liquid N_2 and then the NMR tube was evacuated and sealed. The solution was then thawed and the NMR tube backfilled with ^{13}CO (2 bar) and the resulting mixture allowed to react for 30 min. The vacuum/CO cycle was repeated twice more to ensure that all the ^{12}CO had been displaced. The volatiles were removed under reduced pressure to yield a yellow solid that turned red under prolonged exposure to vacuum. The product was identified in solution by NMR only. The ^1H NMR spectrum of **2b*** was essentially the same as for **2b**. $^{31}P\{H\}$ NMR (121 MHz, $C_6D_5CD_3$, −90 °C): δ 77.9 (dd, $^1J(PPt)$ = 3556 Hz, $^2J(PP)$ = 93 Hz, $^2J(PC)$ = 52 Hz), 76.4 (dd, $^1J(PPt)$ = 3250 Hz, $^2J(PP)$ = 93 Hz, $^2J(PC)$ = 41 Hz). $^{13}C\{H\}$ NMR (75 MHz, $C_6D_5CD_3$, −90 °C): δ 234.6 (dd, $^1J(CPt)$ = 2189 Hz $^2J(PC)$ = 41 Hz, $^2J(PC)$ = 52 Hz, CO).

Preparation of [Pt(L$_a$)(CO)$_2$] (3a)

A solution of **2a** (10.2 mg, 0.0165 mmol) in d_8-toluene (1 mL) was placed in a valved NMR tube. The solution was frozen with liquid N_2 and then the NMR tube was evacuated and sealed. The solution was then thawed and the NMR tube backfilled with CO (2 bar) and the resulting mixture allowed to react for 30 min. The product was not isolated because it reverted to **2a** upon removal of solvent and was identified in solution by NMR. $^{31}P\{H\}$ NMR (121 MHz, $C_6D_5CD_3$, −90 °C): δ 35.3 (s, $^1J(PPt)$ = 3107 Hz). ^1H NMR (300 MHz, $C_6D_5CD_3$): δ 7.1 (m, 2H), 6.9 (m, 2H), 3.3 (br, 4H, CH_2), 1.2 (m, 36H, CCH_3). $^{13}C\{H\}$ NMR (100 MHz, $C_6D_5CD_3$): δ 142.9 (s), 138.7 (s), 130.5 (s), 41.8 (br, CH_2), 37.3 (br, CCH_3), 34.8 (m, CCH_3). ν_{CO} 1971, 1931 cm^{-1}.

Preparation of [Pt(L$_a$)(^{13}CO)$_2$] (3a*)

A solution of **2a** (10.0 mg, 0.0162 mmol) in d_8-toluene (1.2 mL) was placed in a valved NMR tube. The solution was frozen with liquid N$_2$ and then the NMR tube was evacuated and sealed. The solution was then thawed and the NMR tube backfilled with ^{13}CO (2 bar) and the resulting mixture allowed to react for 30 min. The vacuum/CO cycle was repeated twice more to ensure that most of the ^{12}CO had been displaced. The solution was then saturated with N$_2$ to remove the excess of ^{13}CO. The product was not isolated because it reverted to **2a*** upon removal of solvent and was identified in solution by NMR. The ^{1}H NMR spectrum of **3a*** was essentially the same as for **3a**. ^{31}P{H} NMR (121 MHz, C$_6$D$_5$CD$_3$, −90 °C): δ 35.3 (m, ^1J(PPt) = 3107 Hz). ^{13}C{H} NMR (75 MHz, C$_6$D$_5$CD$_3$, −90 °C): δ 187.1 (m, ^1J(CPt) = 1832 Hz, CO) 186.6 (m, ^1J(CPt) = 1900 Hz, CO).

Preparation of [Pt(L$_b$)(CO)$_2$] (3b)

A solution of **2b** (8.7 mg, 0.014 mmol) in d_8-toluene (1 mL) was placed in a valved NMR tube. The solution was frozen with liquid N$_2$ and then the NMR tube was evacuated and sealed. The solution was then thawed and the NMR tube backfilled with CO (2 bar) and the resulting mixture allowed to react for 30 min. The product was not isolated because it reverted to **2b** upon removal of solvent and was identified in solution by NMR. ^{31}P{H} NMR (202 MHz, C$_6$D$_6$): δ 44.4 (d, ^1J(PPt) = 3106 Hz, ^2J(PP) = 20 Hz), 42.7 (d, ^1J(PPt) = 3818 Hz, ^2J(PP) = 20 Hz). ^{1}H NMR (300 MHz, C$_6$D$_5$CD$_3$): δ 7.8 (m, 1H), 7.0 (m, 2H), 6.9 (m, 1H), 3.2 (m, 2H, CH$_2$), 1.3 (d, ^3J(PH) = 13 Hz, 18H, CCH$_3$), 1.1 (d, ^3J(PH) = 13 Hz, 18H, CCH$_3$). ^{13}C{H} NMR (126 MHz, C$_6$D$_6$): δ 143.8 (d, J(CP) = 15 Hz), 134.5 (dd, J(CP) = 8 Hz, J(CP) = 5 Hz), 134.4 (d, J(CP) = 2 Hz), 129.0 (s), 125.4 (s), 124.3 (s), 36.9 (m, CCH$_3$), 34.8 (m, CCH$_3$), 32.4 (m, CCH$_3$), 30.1 (br, CH$_2$), 29.8 (m, CCH$_3$), 28.8 (d, CCH$_3$). ν_{CO} 1961, 1915 cm^{-1}.

Preparation of [Pt(L$_b$)(^{13}CO)$_2$] (3b*)

A solution of **2b** (9.9 mg, 0.0164 mmol) in d_8-toluene (1.2 mL) was placed in a valved NMR tube. The solution was frozen with liquid N$_2$ and then the NMR tube was evacuated and sealed. The solution was then thawed and the NMR tube backfilled with ^{13}CO (2 bar) and then the resulting mixture allowed to react for 30 min. The vacuum/CO cycle was repeated twice more to ensure that all ^{12}CO had been displaced. The product was not isolated because it reverted to **2b*** upon removal of solvent and was identified in solution by NMR. The ^{1}H NMR spectrum of **3b*** was essentially the same as for **3b**. ^{31}P{H} NMR (121 MHz, C$_6$D$_5$CD$_3$, −90 °C): δ 43.0 (m, ^1J(PPt) = 3046 Hz), 40.3 (m ^1J(PPt) = 2788 Hz). ^{13}C{H} NMR (75 MHz, C$_6$D$_5$CD$_3$, −90 °C): δ.187.1 (m, ^1J(CPt) = 1903 Hz, CO), 186.0 (m, ^1J(CPt) = 1850 Hz, CO).

Preparation of [Pt(L$_a$)(C$_2$H$_4$)] (4a)

A solution of **2a** (12.2 mg, 0.0194 mmol) in d_6-benzene (1.2 mL) was placed in a valved NMR tube. The solution was frozen with liquid N$_2$ and then the NMR tube was evacuated and sealed. The solution was then thawed and the NMR tube backfilled with C$_2$H$_4$ (2 bar) and the resulting mixture allowed to react for 30 min. The vacuum/C$_2$H$_4$ cycle was repeated twice more to ensure that most of the CO had been displaced. The product was identified by comparison of its NMR spectra with the literature data for this previously reported complex.[19] ESI mass spectrum: (calcd for C$_{26}$H$_{48}$P$_2$Pt 617.3) M_r − 617.3. ^{31}P{H} NMR (121 MHz, C$_6$D$_6$): δ 48.9 (^1J(PPt) = 3548 Hz). ^{1}H NMR (300 MHz, C$_6$D$_6$): δ 7.1–6.9 (m, 4H), 3.4 (br, 4H, PCH$_2$), 2.2 (br, ^2J(PtH) = 54 Hz, 4H, PtCH$_2$), 1.3 (d, ^3J(PH) = 13 Hz, 36H, CH$_3$).

Reaction of [Pt(L$_b$)(CO)] with ethene

A solution of **2b** (10.6 mg, 0.0175 mmol) in d_8-toluene (1.2 mL) was placed in a valved NMR tube. The solution was frozen with liquid N$_2$ and then the NMR tube was evacuated and sealed. The solution was then thawed and the NMR tube backfilled with C$_2$H$_4$ (2 bar) and the resulting mixture allowed to react for 30 min. The solution was frozen with liquid N$_2$ and then the NMR tube was evacuated and sealed. The solution was then thawed and the NMR tube backfilled with C$_2$H$_4$ (2 bar) and then the resulting mixture allowed to react for 30 min. The vacuum/C$_2$H$_4$ cycle was repeated twice. The product was a mixture of **2b**, **3b** and a species tentatively assigned to **4b** on the basis of its ^{31}P NMR parameters. ^{31}P{H} NMR (121 MHz, C$_6$D$_5$CD$_3$): 60.9 (d, ^1J(PPt) = 3288 Hz, ^2J(PP) 45 Hz), 57.9 (d, ^1J(PPt) = 3288 Hz, ^2J(PP) = 45 Hz).

Preparation of [Pt(L$_a$)(H)(CO)][B(C$_6$F$_5$)$_4$] (5a)

A solution of [(Et$_2$O)$_2$H][B(C$_6$F$_5$)$_4$] (13.8 mg, 0.0166 mmol) in chlorobenzene (0.5 mL) was added in one portion to a solution of **2a** (10.5 mg, 0.0169 mmol) in chlorobenzene (0.5 mL) and the resulting mixture was left for 16 h. The solution was layered with pentane (3 mL) resulting in the slow formation of colourless crystals suitable for X-ray crystallography (14.8 mg, 0.012 mmol, 71%). ESI accurate mass spectrum: (calcd for C$_{25}$H$_{44}$OP$_2$Pt 618.6655) M_r − 618.2589. IR: ν_{CO} 2092 cm^{-1}. Satisfactory C, H elemental analyses for **5a** were not obtained even when a sample from the crystals used for the X-ray crystallography were submitted. ^{31}P{H} NMR (162 MHz, CD$_2$Cl$_2$): δ 43.4 (d, ^1J(PPt) = 2994 Hz, ^2J(PP) = 19 Hz), 34.2 (d, ^1J(PPt) = 2018 Hz, ^2J(PP) = 19 Hz). ^{1}H NMR (400 MHz, CD$_2$Cl$_2$): δ 7.4 (m, 2H), 7.3 (m, 2H), 3.9 (br, 4H, CH$_2$), 1.4 (m, 36H, CCH$_3$), −4.7 (dd, ^2J(PH) = 145 Hz, ^2J(PH) = 15 Hz, ^1J(PtH) = 736 Hz, 1H, PtH). ^{11}B{H} NMR (128 MHz, CD$_2$Cl$_2$): δ −17.7 (s). ^{19}F NMR (376 MHz, CD$_2$Cl$_2$): δ −133.0 (m, 8F, o-C$_6$F$_5$), −162.3 (t, 4F, p-C$_6$F$_5$), 166.2 (m, 8F, m-C$_6$F$_5$).

Preparation of [Pt(L$_b$)(CO)(H)][B(C$_6$F$_5$)$_4$] (5b/6b)

A solution of [(Et$_2$O)$_2$H][B(C$_6$F$_5$)$_4$] (12.5 mg, 0.0151 mmol) in PhCl (0.5 mL) was added in one portion to a solution of **2b** (9.2 mg, 0.015 mmol) in PhCl (0.5 mL) and the resulting mixture was left for 16 h. The solution was layered with pentane (3 mL) to give colourless crystals (17.8 mg, 0.014 mmol, 93%). The product was a mixture of 2 geometric isomers. ^{31}P{H} NMR (202 MHz, CD$_2$Cl$_2$): δ 54.9 (d, ^1J(PPt) = 2948 Hz, ^2J(PP) = 22 Hz), 53.5 (d, ^1J(PPt) = 2978 Hz, ^2J(PP) = 22 Hz) 49.8 (d, ^1J(PPt) = 1879 Hz, ^2J(PP) = 22 Hz), 49.7 (d, ^1J(PPt)

= 1918 Hz, $^2J(PP)$ = 22 Hz). ^{1}H NMR (500 MHz, CD_2Cl_2): δ 8.1 (m, 1H), 7.6 (m, 2H), 7.5 (m, 1H), 3.6 (m, 2H, CH_2), overlapping ^tBu peaks: 1.5 (d, $^3J(PH)$ = 15 Hz, CH_3) 1.5 (d, $^3J(PH)$ = 16 Hz, CH_3) (total integration 18H), overlapping ^tBu peaks: 1.3 (d, $^3J(PH)$ = 15 Hz, CH_3) 1.3 (d, $^3J(PH)$ = 16 Hz, CH_3) (total integration 18H), −2.3 (dd, $^1J(PtH)$ = 777 Hz, $^2J(PH)$ = 147 Hz, $^2J(PH)$ = 11 Hz, 0.2H, PtH), −4.3 (dd, $^1J(PtH)$ = 810 Hz, $^2J(PH)$ = 148 Hz, $^2J(PH)$ = 10 Hz, 0.8H, PtH). $^{11}B\{H\}$ NMR (128 MHz, CD_2Cl_2): δ −16.69 (s). ^{19}F NMR (376 MHz, CD_2Cl_2): δ −133.16 (m, 8F, o-C_6F_5), −163.63 (t, 4F, p-C_6F_5), 167.51 (m, 8F, m-C_6F_5). ESI accurate mass spectrum: (calcd for $C_{24}CH_{43}OP_2Pt$ 604.2431) M_r – 604.2429. Elemental analysis (calcd for $C_{48}H_{43}BF_{20}OP_2Pt$, PhCl): C: 46.65 (46.45) H: 3.10 (3.47). ν_{CO} 2102, 2094 cm^{-1}.

Crystal structure determination

A single crystal of **5a** was mounted on a glass fibre and X-ray diffraction data were collected at 100 K on a Bruker APEX II CCD diffractometer using graphite monochromatised Mo-K$_\alpha$ radiation (λ = 0.71073 Å). Absorption corrections were based on equivalent reflections using SADABS.[27] The structure was solved by direct methods in SHELXS and refined by full matrix least squares on F^2 in SHELXL.[28] All of the non-hydrogen atoms were refined anisotropically and all of the hydrogen atoms were located geometrically and refined using a riding model with the exception of H1D, H1E, H2D, H2E. The structure showed a small amount of disorder in the positions of the CO group and hydride attached to the Pt metal centres. The occupancy of each CO group was determined by refining them against a free variable with the sum of the occupancies for the

two CO sites attached to each Pt set to equal one, prior to fixing the occupancy at the refined values. The hydrogen atoms (H1D, H1E, H2D, H2E) were located on the basis of chemical knowledge and their occupancy fixed to that of the related CO occupancy. Restraints were applied to maintain chemically sensible geometries (DFIX, SADI, DANG) for the disordered sections, while the CO thermal parameters were restrained to similar values using SIMU and the H U_{iso} values was fixed at 1.5 × $U_{eq}(Pt)$. Crystal structure and refinement data are given in Table 1.

Table 1 Crystal data and structure refinement for **5a**

Empirical formula	$C_{49}H_{45}BF_{20}OP_2Pt$
Formula weight	1297.69
Temperature/K	100(2)
Crystal system	Triclinic
Space group	$P\bar{1}$
a/Å	14.3193(7)
b/Å	15.3989(8)
c/Å	23.2615(11)
α/°	93.138(4)
β/°	106.589(4)
γ/°	90.129(4)
Volume/Å^3	4907.5(4)
Z	2
ρ_{calc}/g cm^{-3}	1.756
μ/mm^{-1}	3.039
$F(000)$	2560.0
Crystal size/mm^3	0.10 × 0.15 × 0.17
Radiation	MoKα (λ = 0.71073)
2θ range for data collection/°	3.01 to 51.36
Index ranges	−17 ≤ h ≤ 17, −18 ≤ k ≤ 18, −28 ≤ l ≤ 28
R_{int}	0.1485
Reflections collected	53729
Independent reflections	17 979
Data/restraints/parameters	17 979/76/1406
Goodness-of-fit on F^2	0.981
Final R indexes [$I \geq 2\sigma(I)$]	R_1 = 0.0789, wR_2 = 0.1490
Final R indexes [all data]	R_1 = 0.1799, wR_2 = 0.1877
Largest diff. peak/hole/e Å^{-3}	1.62/−1.61

References

1 C. J. Moulton and B. L. Shaw, *J. Chem. Soc., Chem. Commun.*, 1976, 365.

2 N. Carr, B. J. Dunne, A. G. Orpen and J. L. Spencer, *J. Chem. Soc., Chem. Commun.*, 1988, 926.

3 L. Mole, J. L. Spencer, N. Carr and A. G. Orpen, *Organometallics*, 1991, **10**, 49.

4 (a) R. F. M. J. Parton and M. C. C. Janssen, WO2013030344 (A1), 2013; (b) R. P. Tooze, G. R. Eastham, W. Keith and X. L. Wang, WO9619434 (A1), 1996; (c) J. M. Pearson and R. A. Hadden, WO9841495 (A1), 1998; (d) J. G. De Vries, N. Sereinig, E. W. M. Van de Vondervoort and M. C. C. Janssen, WO2012131027 (A1), 2012; (e) G. R. Eastham, R. P. Tooze, X. L. Wang and K. Whiston, US6335471 (B1), 1996; (f) W. Clegg, M. R. J. Elsegood, G. R. Eastham, R. P. Tooze, X. Lan Wang and K. Whiston, *Chem. Commun.*, 1999, 1877.

5 (a) R. I. Pugh, E. Drent and P. G. Pringle, *Chem. Commun.*, 2001, 1476; (b) S. Doherty, E. G. Robins, J. G. Knight, C. R. Newman, B. Rhodes, P. A. Champkin and W. Clegg, *J. Organomet. Chem.*, 2001, **640**, 182; (c) J. G. Knight, S. Doherty, A. Harriman, E. G. Robins, M. Betham, G. R. Eastham, R. P. Tooze, M. R. J. Elsegood, P. Champkin and W. Clegg, *Organometallics*, 2000, **19**, 4957; (d) O. V. Gusev, A. M. Kalsin, M. G. Peterleitner, P. V. Petrovskii, K. A. Lyssenko, N. G. Akhmedov, C. Bianchini, A. Meli and W. Oberhauser, *Organometallics*, 2002, **21**, 3637; (e) C. Bianchini, A. Meli, W. Oberhauser, M. A. Zuideveld, Z. Freixa, P. C. J. Kamer, A. L. Spek, O. V. Gusev and A. M. Kal'sin, *Organometallics*, 2003, **22**, 2409; (f) O. V. Gusev, A. M. Kalsin, P. V. Petrovskii, K. A. Lyssenko, Y. F. Oprunenko, C. Bianchini, A. Meli and W. Oberhauser, *Organometallics*, 2003, **22**, 913; (g) N. R. Vautravers and D. J. Cole-Hamilton, *Dalton Trans.*, 2009, 2130; (h) E. Drent, J. A. M. Van Broekhoven and M. J. Doyle, *J. Organomet. Chem.*, 1991, **417**, 235; (i) S. J. Dossett, A. Gillon, A. G. Orpen, J. S. Fleming, P. G. Pringle, D. F. Wass and M. D. Jones, *Chem. Commun.*, 2001, 699; (j) C. Bianchini, H. M. Lee, A. Meli, S. Moneti, F. Vizza, M. Fontani and P. Zanello, *Macromolecules*, 1999, **32**, 4183; (k) C. Bianchini, H. Man Lee, P. Barbaro, A. Meli, S. Moneti and F. Vizza, *New J. Chem.*, 1999, **23**, 929; (l) E. Lindner, M. Schmid, J. Wald, J. A. Queisser,

M. Geprägs, P. Wegner and C. Nachtigal, *J. Organomet. Chem.*, 2000, **602**, 173; (*m*) P. W. N. M. van Leeuwen, M. A. Zuideveld, B. H. G. Swennenhuis, Z. Freixa, P. C. J. Kamer, K. Goubitz, J. Fraanje, M. Lutz and A. L. Spek, *J. Am. Chem. Soc.*, 2003, **125**, 5523.

6 (*a*) G. R. Eastham, B. T. Heaton, J. A. Iggo, R. P. Tooze, R. Whyman and S. Zacchini, *Chem. Commun.*, 2000, 609; (*b*) W. Clegg, G. R. Eastham, M. R. J. Elsegood, B. T. Heaton, J. A. Iggo, R. P. Tooze, R. Whyman and S. Zacchini, *Organometallics*, 2002, **21**, 1832.

7 J. Wolowska, G. R. Eastham, B. T. Heaton, J. A. Iggo, C. Jacob and R. Whyman, *Chem. Commun.*, 2002, 2784.

8 T. Fanjul, G. Eastham, N. Fey, A. Hamilton, A. G. Orpen, P. G. Pringle and M. Waugh, *Organometallics*, 2010, **29**, 2292.

9 T. Fanjul, G. Eastham, M. F. Haddow, A. Hamilton, P. G. Pringle, A. G. Orpen, T. P. W. Turner and M. Waugh, *Catal. Sci. Technol.*, 2012, **2**, 937.

10 V. de la Fuente, M. Waugh, G. R. Eastham, J. A. Iggo, S. Castillón and C. Claver, *Chem. – Eur. J.*, 2010, **16**, 6919.

11 T. Fanjul, G. Eastham, J. Floure, S. J. K. Forrest, M. F. Haddow, A. Hamilton, P. G. Pringle, A. G. Orpen and M. Waugh, *Dalton Trans.*, 2013, **42**, 100.

12 P. G. Edwards, J. C. Knight and P. D. Newman, *Dalton Trans.*, 2010, **39**, 3851.

13 S. Bertsch, H. Braunschweig, M. Forster, K. Gruss and K. Radacki, *Inorg. Chem.*, 2011, **50**, 1816 and references therein.

14 E. Nicolas, G. Nocton and N. Mezailles, *Eur. J. Inorg. Chem.*, 2013, 4000.

15 (*a*) P. Chini and G. Longoni, *J. Chem. Soc. A*, 1970, 1542; (*b*) G. K. Anderson, H. C. Clark and J. A. Davies, *Organometallics*, 1982, **1**, 550; (*c*) V. V. Grushin, I. S. Akbem and M. E. Vol'pin, *J. Organomet. Chem.*, 1989, **371**, 403; (*d*) P. Giannocaro, A. Sacco and G. Vasapollo, *Inorg. Chim. Acta*, 1979, **31**, L455; (*e*) R. S. Paonessa and W. C. Trogler, *J. Am. Chem. Soc.*, 1982, **104**, 1138.

16 G. K. Anderson, G. J. Lumetta and J. W. Siria, *J. Organomet. Chem.*, 1992, **434**, 253.

17 T. Yoshida, T. Yamagata, T. H. Tulip, J. A. Ibers and S. Otsuka, *J. Am. Chem. Soc.*, 1978, **100**, 2063.

18 B. L. Bennett and D. M. Roddick, *Inorg. Chem.*, 1996, **35**, 4703.

19 N. Carr, L. Mole, A. G. Orpen and J. L. Spencer, *J. Chem. Soc., Dalton Trans.*, 1992, 2653.

20 P. Jutzi, C. Muller, A. Stammler and H.-G. Stammler, *Organometallics*, 2000, **19**, 1442.

21 D. Vuzman, E. Poverenov, Y. Diskin-Posner, G. Leitus, L. J. W. Shimon and D. Milstein, *Dalton Trans.*, 2007, 5692.

22 F. H. Allen, *Acta Cryst.*, 2002, **B58**, 380.

23 P. G. Edwards, J. C. Knight and P. D. Newman, *Dalton Trans.*, 2010, **39**, 3851.

24 T. Weisheit, H. Petzold, H. Gorls, G. Mloston and W. Weigand, *Eur. J. Inorg. Chem.*, 2009, 3545.

25 M. F. Ernst and D. M. Roddick, *Organometallics*, 1990, **9**, 1586.

26 S. Ogoshi, M. Morita, K. Inoue and H. Kurosawa, *J. Organomet. Chem.*, 2004, **689**, 662.

27 Bruker, *SADAB-2012/1, Absorption Correction*, Bruker AXS Inc., Madison, Wisconsin, USA, 2012.

28 G. M. Sheldrick, *Acta Crystallogr., Sect. A: Fundam. Crystallogr.*, 2008, **64**, 112.